Translational Oncology
www.transonc.com

Volume 11 Number 3 June 2018 pp. 700–714 700

Identification of Prognostic Biomarkers by Combined mRNA and miRNA Expression Microarray Analysis in Pancreatic Cancer

Bin Liu*, Hai Yang*, Leila Taher†, Axel Denz*, Robert Grützmann*, Christian Pilarsky* and Georg F. Weber*

*Department of Surgery, Universitätsklinikum Erlangen, Krankenhausstraße 12, Erlangen, Germany; †Division of Bioinformatics, Department of Biology, Friedrich-Alexander Universität Erlangen-Nürnberg, 91054 Erlangen, Germany

Abstract

Pancreatic cancer is the fourth leading cause for cancer-related death, and early diagnosis is one key to improve the survival rate of this disease. Molecular biomarkers are an important method for diagnostic use in pancreatic cancer. We used data from three mRNA microarray datasets and a microRNA dataset (GSE16515, GSE15471, GSE28735, and GSE41372) to identify potential key genes. Differentially expressed genes (DEGs) and microRNAs (DEMs) were identified. Functional, pathway enrichment, and protein-protein interaction analyses were performed on common DEGs across all datasets. The target genes of the DEMs were identified. DEMs targets that were also DEGs were further scrutinized using overall survival analysis. A total of 236 DEGs and 21 DEMs were identified. There were a total of four DEGs (ECT2, NR5A2, NRP2, and TGFBI), which were also predicted target genes of DEMs. Overall survival analysis showed that high expression levels of three of these genes (ECT2, NRP2, and TGFBI) were associated with poor overall survival for pancreatic cancer patients. The basic expression of DEGs in pancreas stood lower level in various organ tissues. The expression of ECT2 and NRP2 was higher in different pancreatic cancer cell lines than normal pancreas cell line. Knockout of ECT2 by Crispr Cas9 gene editing system decreased proliferation and migration ability in pancreatic cancer cell line MiaPaCa2. In conclusion, we think that data mining method can do well in biomarker screening, and ECT2 and NRP2 can play as potential biomarker or therapy target by Crispr Cas9 in pancreatic cancer.

Translational Oncology (2018) 11, 700–714

Introduction

Pancreatic cancer is one of the few cancer types where the 5-year survival rate shows no improvement [1]. In 2016 in the United States, pancreatic cancer was diagnosed in approximately 53,070 patients and caused an estimated 41,780 deaths [2]. In China, the incidence of pancreatic cancer was in an upward trend from 2000 to 2011, and pancreatic cancer is one of the top 10 most common cancers in both men and women [3]. In Europe, pancreatic cancer is currently one of the most lethal types of cancer and has a 5-year survival of approximately 7% [2]. It is expected to rise to second place behind lung cancer by 2030 [4]. Surgery is currently the only potentially curative treatment for pancreatic cancer [5]. However, pancreatic surgery in early state is associated with significant morbidity and mortality [6]. The poor prognosis of pancreatic cancer is mainly attributed to rapid disease progression; late diagnosis at advanced, unresectable stages; and inadequate response to current adjuvant or palliative regimens. Indeed, there is no effective diagnostic method at early stage, and most pancreatic cancer patients are first diagnosed at advanced stages [7,8].

High-throughput technologies combined with vast amounts of publicly available data and sophisticated online analysis tools enable the scientific community to mine knowledge about genes related to cancer development in an unprecedented manner. Different types of molecular biomarkers can be used for diagnosis, prognosis, and

Address all correspondence to Christian Pilarsky, Department of Surgery, Universitätsklinikum Erlangen, Krankenhausstraße 12, Erlangen, Germany.
E-mail: christian.pilarsky@uk-erlangen.de
Received 23 January 2018; Revised 7 March 2018; Accepted 12 March 2018

1936-5233/18
https://doi.org/10.1016/j.tranon.2018.03.003

prediction and monitoring of response to treatment. For example, the presence or absence or changes in the level of specific biomarkers in a cell are routinely used as an indication of cancer development. Molecular biomarkers are an important diagnosis tool in pancreatic cancer [9]. Thus, multiple studies have confirmed that carbohydrate antigen 19-9 (CA 19-9) and carcinoembryonic antigen (CEA) can be used to predict the outcomes of multiple diseases, including pancreatic cancer [10–12]. However, these biomarkers are not sufficiently specific or sensitive for use in pancreatic cancer [13,14]. The identification of novel pancreatic cancer-specific molecular biomarkers is crucial for early effective diagnosis [15].

Microarrays, including DNA, microRNA, protein, and antibody microarrays, are a multiplex lab-on-a-chip system. More specifically, a microarray is a 2D array on a solid substrate for assaying large amounts of biological material using miniaturized, multiplexed, and parallel processing and detection methods. Microarrays are widely used in biomedical research. For instance, they have been used to infer general genetic alterations during tumorigenesis [16]. Microarray data are also the main resources of biomarker candidates [17]. In this study, we integrated data from three mRNA microarray datasets and a microRNA dataset with pathway, functional, and overall survival analysis to identify putative novel pancreatic cancer biomarkers among differentially expressed genes (DEGs) and microRNAs (DEMs) between normal and pancreatic cancer tissue. Crispr Cas9 system has led a revolution in gene editing. Our laboratory has done a lot of work on this field with wealth of experience. In this study, we verified the data mining results by Crispr Cas9 gene editing system and other experiments.

Materials and Methods

Microarray Datasets and Data Processing

We selected and downloaded three human pancreatic cancer gene expression (GSE16515 [18], GSE15471 [19], and GSE28735 [20,21]) and one human pancreatic cancer miRNA expression (GSE41372 [22]) datasets from the Expression Omnibus database (GEO) [23]. The three gene expression datasets include 117 cancer tissue samples and 97 normal tissue samples from 117 pancreatic cancer patients. The miRNA dataset comprises pancreatic ductal adenocarcinoma tumor samples from nine patients and normal pancreas samples from nine healthy individuals. All these datasets were generated on Affymetrix chips and uploaded by independent groups. The GSE16515 and GSE15471 datasets are based on the GPL570 platform; the GSE28735 and GSE41372 datasets are based on the GPL16142 platform. These platforms are the mainstream choice for biomarker research [24].

We used GEO2R [25] to identify DEGs and DEMs between pancreatic cancer and normal tissue samples. GEO2R is an online tool which can compare different groups in a GEO series. The pancreatic cancer samples served as the "cancer group," and the normal samples as the "control group." We selected genes whose adjusted (Benjamini & Hochberg or false discovery rate [26]) *P* value was smaller than .01 and with an absolute log fold-change greater than 1.

We used the online tool "Calculate and draw custom Venn diagrams" (http://bioinformatics.psb.ugent.be/webtools/Venn/) to identify genes that were up- or downregulated in all three GEO datasets.

Gene Function and Pathway Enrichment Analysis

We used the Database for Annotation, Visualization, and Integrated Discovery (DAVID [27]) to perform a functional enrichment analysis of the DEGs. DAVID is an online program to help understand biological meaning behind plenty of genes with comprehensive function, including the Gene Ontology (GO) and Kyoto Encyclopedia of Genes and Genomes (KEGG) pathway enrichment analysis. We set the cutoff criterion $P < .05$ of false discovery rate.

Protein-Protein Interaction (PPI) Network Construction and Module Analysis

We used the Search Tool for the Retrieval of Interacting Genes (STRING) database to analyze functional interactions between proteins [28]. We retrieved interactions with confidence scores greater or equal to 0.7 and screened the resulting PPI network for modules with Cytoscape-MCODE [29] and the following parameters: degree cutoff=2, node score cutoff=0.2, k-core=0.2, and maximum depth=100.

Prediction of miRNA Targets

We used GEO2R to identify DEMs between pancreatic cancer and normal tissue samples. The pancreatic cancer samples served as the "cancer group" and the normal samples as the "control group." We selected miRNAs whose adjusted (Benjamini & Hochberg or false discovery rate [26]) *P* value was smaller than .01 and with an absolute log fold-change greater than 1. We used the "miRecords" tool to predict miRNA target genes [30]. miRecords integrates the results of more than 10 miRNA target prediction programs. No target was predicted for more than six miRNA target prediction programs, so we only considered DEM target genes predicted by exactly six prediction programs. Finally, we used the online tool "Calculate and draw custom Venn diagrams" (http://bioinformatics.psb.ugent.be/webtools/Venn/) to identify common target DEGs of for the DEMs.

Survival Analysis of DEGs

We used the OncoLnc tool (www.oncolnc.org) [31] to perform overall survival analysis in pancreatic cancer. OncoLnc is an online tool for interactively exploring survival correlations. It contains survival data for 8647 patients from 21 cancer studies in The Cancer Genome Atlas (TCGA), along with RNA-seq data for mRNA and miRNA expression from TCGA, and lncRNA expression from MiTranscriptome beta. The tool gives the user the ability to separate patients based on the gene expression level of a specific gene and create Kaplan-Meier plots. We recorded hazard ratios with their 95% confidence intervals and log-rank *P* values. Top 10, 20, and 40 and bottom 90, 80, and 60 percentiles of expression values, respectively, were considered as high and low groups. Additionally, OncoLnc was used to do the overall survival analysis for other cancer types, including breast, lung, gastric, and liver cancer.

The Basic Expression of DEGs in Different Organs and Cancer Tissues

We used the online tool " The Human Protein Atlas " to perform the basic expression level of DEGs in different human organs. The Human Protein Atlas is a Swedish-based program started in 2003. We worked with version 17 in this study, which was launched in August 2017 [32]. In the Tissue Atlas part, it shows the distribution of the proteins across all major tissues and organs in human. There

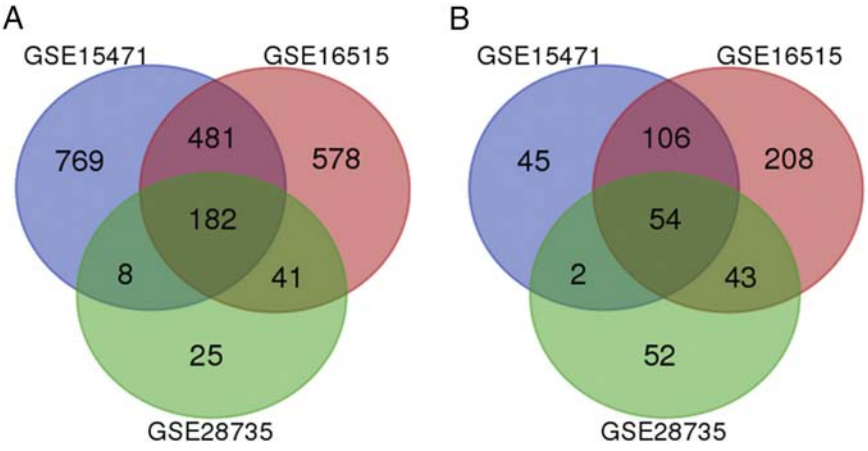

Figure 1. Identification of DEGs in mRNA expression profiling datasets GSE15471, GSE16515, and GSE28735. (A) The upregulated genes in the profiling datasets. (B) The downregulated genes in the profiling datasets.

were three datasets in the website: HPA dataset (RNA-seq tissue data are reported as mean transcripts per million, corresponding to mean values of the different individual samples from each tissue), GTEx dataset (RNA-seq data are reported as median reads per kilobase per million mapped reads, generated by the Genotype-Tissue Expression project), and FANTOM5 dataset (tissue data obtained through cap analysis of gene expression are reported as tags per million, generated by the FANTOM5 project). We used them together in this study. In additional, we also conducted the different expression between normal pancreas and pancreatic cancer tissues. UALCAN is an easy-to-use online tool for in-depth analyses of TCGA gene expression data. It uses TCGA level 3 RNA-seq and clinical data from 31 cancer types. In this study, we used it to identify the up- or downregulated of DEGs in pancreatic cancer.

Cell Culture

In this study, we used human pancreatic cancer lines ASPC1, BXPC3, PANC1, HS766T, and MiaPaCa 2; primary cell lines PaCaDD119, PaCaDD137, and PaCaDD159; and normal pancreas cell line HDPE. ASPC1, BXPC3, PANC1, HS766T, MiaPaCa 2, and HDPE were purchased from ATCC, and all the cells were grown in monolayer culture in a humidified atmosphere containing 5% CO2 at 37°C. The culture medium for ASPC1, BXPC3, and PANC1 consists of RPMI Medium 1640 (Gibco, 21875-034) with 10% FBS (Gibco, A31608-01). HS766T cell was cultured in DMEM (Gibco, 30966-021) with 10% FBS. MiaPaCa 2 cell was cultured in DMEM with 10% FBS and 2% horse serum (Gibco, 16050-130). HDPE cell was cultured in Keratinocyte-SFM (Gibco, 10724-011). PaCaDD119, PaCaDD137, and PaCaDD159 were cultured in mixed medium with 53.5% DMEM, 13.2% FBS, and 33.3% Keratinocyte-SFM. All cells were harvested by 0.25% Trypsin-EDTA (Gibco, 25200-072).

Western Blot

Cells were lysed with RIPA buffer. Gel electrophoresis was performed under reducing conditions with acrylamide gel, and proteins were transferred to a nitrocellulose membrane. As primary antibodies, ECT2 (Merck Millipore, 07-1364), NRP2 (Cell Signaling Technology, 3366), and TGFBI (Thermo Fisher Scientific, PA5-19242) were used for detection. The GAPDH (Cell Signaling Technology, 5175S) served as loading control. HRP-linked anti-rabbit IgG (Cell Signaling Technology, 7074) was used as second antibody. Quantification of signal was performed by Amersham Imager 600 with SignalFire Elite ECL Reagent (Cell Signaling Technology, 12757S). All Western blot results were done at least two times.

Quantitative RT-PCR

The isolation of RNA was performed with NucleoSpin RNA Plus kit (Macherey-Nagel, #740984.250), and the cDNA was synthesized with High Capacity cDNA Reverse Transcription Kit (Applied Biosystems, 00364942). The quantitative RT-PCR was performed with PowerUP SYBR Green Master Mix (Applied Biosystems, A25741) and analyzed by $2^{-\triangle\triangle Ct}$ method. The GAPDH was used as reference value. Primer sequences for amplification were as follows: ECT2-forward (5′- AGGAGTCGGCGTTTGAAGAG-3′), ECT2-reverse (5′- GGTCCAATAACTCTACAATCAGCC-3′), NRP2-forward (5′- CGCGGAGGAGACAGTATCAC-3′), NRP2-reverse (5′- CCGAAGAGGAGGCCACAGAG-3′), TGFBI-forward (5′- AAGGTAACGGCCAGTACACG-3′), TGFBI-reverse(5′-GAGATGATCGCCTTCCCGTT-3′), GAPDH-forward (5′-CTTTGGTATCGTGGAAGGACTC-3′), GAPDH-reverse(5′-AGTAGAGGCAGGGATGATGT-3′). All primers were synthesized by Eurofins.

CRISPR/Cas9 Gene Editing

In this study, ECT2 was knocked out by CRISPR/Cas9 gene editing in the MiaPaCa2 cell line. The pSpCas9(BB)-2A-GFP (PX458, Plasmid #48138) plasmid was purchase from Addgene. HGLibB-14402-ECT2 sgRNA (forward: 5′- CACCTGTCTTTAATGACCTCTACA -3′ and reverse: 5′-AAACTGTAGAGGTCATTAAAGACA-3′) and Hu-64433nc-sgRNA (forward: 5′-CACCATCGTATCATCAGC-TAGCGC-3′ and reverse: 5′-AAACGCGCTAGCTGATGATAC-GAT-3′) were synthesized by Eurofins. Plasmid construction was done as described in the protocol and confirmed by sequencing. MiaPaCa cells were transfected with ECT2 knockout plasmid by Lipofectamine 3000 Transfection Reagent (Invitrogen, L3000015) as protocol for 72 hours. Then, all the GFP-positive cells were sorted by fluorescence activated cell sorter. Sixty GFP-positive cells were plated in one 96-well plate for selecting single clones. After a few days of culture, Western blot and sequencing were used to make

Table 1. Total 236 Genes Which Showed Consistent Trend in Up- or Downregulation in Three Microarrays Were Considered DEG in GSE15471, GSE16515, and GSE28735 Datasets

Upregulated DEGs						
	GSE15471		GSE16515		GSE28735	
	Adj *P*	Log FC	Adj *P*	Log FC	Adj *P*	Log FC
ABHD17C	6.41e-05	−1.10562734	1.60e-08	−2.895825	3.31e-12	−1.128362
ACSL5	2.43e-03	−1.18356539	1.96e-04	−1.9244909	8.95e-08	−1.4634847
ACTA2	9.91e-06	−1.56347311	4.02e-03	−1.3521614	1.73e-05	−1.1454927
ADAM12	4.08e-08	−1.81573918	2.20e-02	−1.2155662	6.89e-04	−1.0717007
ADAM28	1.00e-07	−1.86173177	3.35e-04	−1.5977978	5.10e-06	−1.141082
ADAM9	2.19e-10	−1.71106472	8.41e-07	−1.8466136	1.74e-07	−1.1530387
ADAMTS12	5.56e-17	−2.42053266	2.20e-04	−1.8683158	3.77e-09	−1.4163264
ADAMTS6	1.14e-08	−1.08645267	2.58e-05	−1.1985481	2.89e-08	−1.038462
ADGRF1	4.41e-06	−1.13978583	2.11e-03	−1.1893599	1.24e-08	−1.6035156
AEBP1	2.36e-16	−2.70716438	1.99e-03	−1.7154245	1.80e-06	−1.1198558
AGR2	1.28e-04	−2.04964413	3.29e-05	−2.7721982	2.25e-10	−2.1373789
AHNAK2	2.75e-13	−2.53976184	2.20e-04	−1.6346964	5.51e-13	−1.7455516
ANKRD22	1.07e-05	−1.30858993	2.94e-07	−2.1128529	1.35e-08	−1.5765009
ANLN	4.03e-06	−1.3095382	1.35e-07	−2.231518	7.00e-09	−1.6620173
ANO1	6.05e-15	−2.97053176	1.59e-04	−1.7574292	2.55e-09	−1.2739089
ANTXR1	1.83e-12	−1.49081539	8.76e-04	−1.218539	7.64e-09	−1.5904338
ANXA10	9.12e-05	−2.00705104	2.49e-04	−3.2509851	7.58e-09	−2.3579367
ANXA3	2.08e-07	−1.49208035	1.47e-06	−1.9301469	4.51e-06	−1.0462073
ANXA8L1///ANXA8	1.24e-05	−1.29098707	1.50e-04	−2.8578011	1.45e-07	−1.4583824
APOL1	2.98e-10	−1.11856761	1.82e-06	−1.9469703	7.27e-10	−1.5050227
AREG	2.33e-06	−1.95574758	2.20e-04	−1.9826671	3.11e-03	−1.0105213
ARNTL2	1.55e-09	−1.43839367	1.05e-06	−1.8453465	1.15e-08	−1.2634424
ASAP2	5.40e-12	−1.27142048	1.25e-06	−1.4437181	1.38e-11	−1.0555331
ASPM	1.34e-05	−1.38313105	4.95e-06	−2.1664253	2.91e-07	−1.2180584
BGN	2.63e-12	−1.61702033	4.83e-03	−1.2980139	5.11e-06	−1.2178456
CAPG	1.74e-16	−2.23018436	8.56e-06	−2.2290411	8.56e-10	−1.409224
CCL18	4.24e-05	−1.50008642	3.09e-03	−1.7869004	1.20e-03	−1.1312298
CCL20	2.65e-06	−2.18836311	9.93e-06	−3.3482898	3.16e-08	−1.3648089
CD109	7.32e-12	−2.35811014	1.96e-04	−1.9508099	2.18e-07	−1.2498704
CDH11	2.09e-11	−1.62227423	8.02e-04	−1.2080804	2.35e-07	−1.4890444
CDH3	4.98e-09	−1.50129524	7.33e-07	−2.6825856	1.81e-12	−1.6362931
CEACAM1	4.36e-05	−1.41621839	2.67e-06	−1.635777	3.37e-09	−1.292694
CEACAM5	7.46e-06	−2.76526848	2.33e-07	−6.2525663	1.07e-10	−3.1812869
CEACAM6	3.73e-08	−3.19875853	2.11e-06	−4.2600263	3.78e-10	−2.6271224
CEMIP	2.81e-07	−2.45896857	4.01e-06	−2.7846301	9.49e-11	−1.8033796
CLDN18	2.91e-04	−1.61076389	2.73e-05	−4.0364872	2.41e-08	−2.1265416
COL10A1	4.79e-18	−4.11443223	1.37e-05	−3.3673523	2.59e-11	−1.5692449
COL11A1	1.24e-07	−1.88113667	1.64e-04	−2.2589512	1.42e-10	−2.1946749
COL12A1	7.24e-08	−1.52434785	3.78e-04	−1.6268338	3.71e-07	−1.732026
COL1A1	8.67e-08	−1.33504418	1.18e-03	−2.0914504	1.80e-05	−1.5020929
COL3A1	5.36e-10	−1.47689589	2.61e-03	−1.2776155	7.92e-05	−1.3701904
COL5A2	4.21e-16	−3.44422932	7.75e-04	−1.8667315	8.85e-06	−1.3867727
COL8A1	1.60e-14	−2.08659948	1.46e-02	−1.0532559	2.56e-07	−1.4414827
COMP	1.60e-14	−3.57453998	3.99e-03	−2.155856	2.08e-06	−1.4673376
CORIN	6.57e-09	−1.80041916	9.81e-04	−1.4909615	7.13e-07	−1.0800867
CP	3.17e-05	−1.38183429	2.07e-02	−1.3531284	3.29e-05	−1.767232
CST1	4.28e-13	−3.34647655	4.61e-04	−3.0382825	2.25e-08	−2.0248356
CST2	4.08e-10	−1.80213342	2.41e-03	−1.2489128	9.70e-09	−1.2321847
CTHRC1	6.72e-17	−4.43075384	2.67e-04	−2.7308879	7.77e-09	−1.0049256
CTSE	3.35e-08	−2.7257767	2.67e-07	−4.6208679	6.93e-12	−2.6841011
CTSK	2.95e-13	−2.61423967	7.83e-03	−1.3986692	2.43e-04	−1.0460687
CXCL5	7.79e-08	−2.4255966	1.03e-04	−3.6610098	1.74e-07	−1.5615738
DCBLD2	1.10e-09	−1.34056587	3.01e-03	−1.111635	3.46e-07	−1.0321687
DDX60	2.29e-08	−1.55703481	3.20e-05	−1.5469602	6.06e-07	−1.0535862
DGKH	5.53e-09	−1.51658317	2.00e-04	−1.3050633	7.09e-07	−1.0501716
DHRS9	1.83e-07	−1.25123427	5.22e-04	−2.4339574	2.72e-06	−1.2735449
DKK1	3.90e-10	−2.30661726	1.03e-06	−3.8761945	2.17e-07	−1.2162724
DLGAP5	1.41e-04	−1.03619236	7.33e-07	−2.0790401	6.75e-07	−1.1127349
DPCR1	2.17e-03	−1.16453163	8.01e-05	−3.7233879	5.55e-08	−2.1386271
DPYSL3	8.50e-12	−2.01701306	4.72e-03	−1.3999587	2.12e-05	−1.1362667
ECT2	2.12e-10	−2.18367354	1.04e-04	−1.2024523	4.55e-10	−1.3293738
EDIL3	3.14e-11	−2.55947048	1.10e-03	−1.5476678	8.64e-07	−1.5138422
EDNRA	1.24e-14	−1.83821405	1.84e-03	−1.3556256	2.52e-07	−1.3127658
EFNA5	1.66e-10	−1.35782403	6.99e-06	−1.3028334	7.69e-10	−1.1553482
EFNB2	1.18e-07	−1.32743105	3.28e-05	−2.038012	2.49e-09	−1.0293451
ENO2	5.56e-10	−1.6129782	9.21e-05	−1.6946701	1.25e-07	−1.1134007
EPHA4	1.75e-08	−1.01758354	2.29e-03	−1.0761163	1.88e-07	−1.1711916
EPYC	1.32e-04	−1.73276174	8.42e-03	−1.9365965	9.64e-04	−1.0430022
ERO1A	1.11e-05	−1.0560388	8.59e-07	−1.9237551	1.17e-09	−1.219264

(continued on next page)

TABLE 1 (*continued*)

	Upregulated DEGs					
	GSE15471		GSE16515		GSE28735	
	Adj *P*	Log FC	Adj *P*	Log FC	Adj *P*	Log FC
ETV1	9.65e-14	−2.3034463	3.70e-04	−1.270131	2.53e-06	−1.0579796
FAP	1.77e-16	−3.38881049	2.81e-03	−1.9046404	1.33e-05	−1.4972633
FBXO32	9.65e-14	−1.72359572	2.45e-03	−1.3835639	2.13e-11	−1.4711818
FCGR3B///FCGR3A	7.76e-08	−2.41674826	6.89e-03	−1.6425105	6.57e-05	−1.0251151
FERMT1	1.64e-06	−1.35306111	4.34e-06	−1.3772776	7.21e-10	−1.5010753
FGD6	1.59e-09	−1.06124145	2.87e-07	−1.6101424	7.37e-10	−1.2339911
FN1	2.54e-10	−1.50889045	2.98e-03	−1.4748314	8.61e-10	−2.2111
FNDC1	2.35e-13	−2.72629222	8.25e-03	−1.6330736	1.79e-06	−1.4763207
FOXQ1	1.99e-07	−1.95639952	2.26e-07	−2.5948572	5.81e-09	−1.1159918
FXYD3	9.25e-07	−1.80033698	2.60e-06	−2.0743889	9.49e-11	−1.5452418
GABRP	4.28e-09	−3.01817945	1.64e-04	−3.6208516	2.95e-06	−2.0308344
GCNT3	5.28e-05	−1.84782101	1.03e-06	−3.3547133	3.12e-06	−1.4315447
GJB2	3.55e-13	−3.69109958	1.68e-07	−3.5861489	2.21e-12	−1.0717644
GPRC5A	1.73e-13	−2.71073028	2.33e-07	−3.7777146	7.88e-10	−1.1751238
GPX2	6.17e-06	−2.06753479	7.71e-03	−1.0570848	1.44e-05	−1.1878256
GPX8	6.62e-13	−1.75319459	4.07e-03	−1.0746134	5.69e-06	−1.0094489
GREM1	8.23e-09	−3.20668556	1.89e-03	−2.0067714	2.56e-07	−1.0603713
HEPH	1.09e-06	−2.04989436	9.21e-04	−2.1788215	2.74e-07	−1.2034709
HK2	7.54e-10	−1.54961514	1.25e-08	−2.7161319	7.91e-09	−1.3526864
IFI27	1.87e-09	−2.24277682	2.33e-07	−3.3295833	3.18e-09	−1.3512633
IFI44L	9.20e-10	−1.99737328	1.04e-03	−2.0539791	1.51e-04	−1.2289118
IGF2BP3	1.63e-07	−1.58746323	1.67e-05	−3.0528705	1.76e-07	−1.1658791
IGFBP5	4.44e-10	−1.00217799	1.31e-03	−1.3627484	2.24e-05	−1.3557069
IL1R2	4.90e-07	−1.65352388	3.00e-04	−2.0617929	1.07e-06	−1.0359142
INPP4B	2.09e-10	−1.61525246	1.07e-03	−1.4033133	5.46e-09	−1.12227
ITGA2	3.03e-12	−1.38190767	1.13e-07	−2.6491086	4.28e-11	−2.2658244
ITGA3	7.36e-09	−1.32864472	1.25e-06	−2.2800449	7.10e-10	−1.5188551
ITGB4	6.66e-09	−1.23313595	2.66e-05	−1.9259157	2.30e-11	−1.303354
KCNN4	1.15e-07	−1.11084866	4.45e-07	−2.2400205	1.59e-14	−1.0487336
KRT19	3.16e-11	−3.71089111	1.61e-08	−4.472929	1.21e-11	−2.0580204
KRT7	1.31e-13	−3.10730417	6.96e-07	−3.2872588	5.98e-07	−1.6835824
KYNU	3.47e-08	−1.17046153	1.57e-04	−1.3876635	1.61e-06	−1.2622391
LAMA3	4.56e-09	−2.25796154	2.83e-03	−1.3755993	8.50e-12	−1.3547947
LAMB3	1.58e-08	−1.7945134	2.96e-10	−3.6738991	1.59e-14	−2.3442298
LAMC2	3.83e-09	−1.59628476	4.14e-07	−3.0935974	1.59e-14	−2.9016536
LCN2	8.46e-09	−2.89069735	6.50e-06	−3.7867526	6.00e-05	−1.1424984
LEF1	2.24e-10	−2.75342766	1.16e-04	−2.4864991	6.33e-09	−1.3104127
LOXL2	1.75e-09	−1.61216046	5.53e-06	−2.2926783	1.28e-08	−1.2380353
LRRN1	2.66e-12	−1.68745871	4.99e-04	−1.5438467	3.21e-06	−1.1022207
MALL	4.20e-05	−1.44176733	4.37e-05	−2.5583935	5.55e-08	−1.0471758
MBOAT2	1.30e-10	−1.12972612	1.27e-06	−1.9018549	1.76e-11	−1.5977576
MELK	4.19e-06	−1.21151988	1.50e-06	−2.0270539	1.38e-07	−1.1532836
MET	2.66e-09	−1.50207236	6.50e-04	−1.1683551	1.20e-09	−1.4803842
MICAL2	1.38e-10	−1.20391622	6.07e-04	−1.1188393	7.99e-11	−1.2684082
MLPH	2.74e-07	−1.47717238	4.75e-07	−2.748077	1.63e-14	−1.4629327
MMP1	2.56e-08	−3.49148002	4.63e-04	−2.9607088	1.36e-03	−1.2251593
MMP11	2.98e-09	−1.96177983	1.92e-05	−2.6722979	2.28e-09	−1.5014524
MMP12	2.52e-06	−2.66435443	5.23e-04	−3.1168124	2.42e-07	−1.7443562
MMP14	9.90e-11	−1.19811673	6.29e-05	−1.222454	9.99e-09	−1.325874
MMP7	6.50e-11	−3.37196074	8.22e-04	−2.4186142	1.57e-03	−1.2129338
MMP9	7.76e-04	−1.25841013	5.39e-04	−1.7459301	2.83e-07	−1.1166764
MTMR11	2.59e-08	−1.73578547	4.71e-06	−2.3963792	9.96e-11	−1.1160298
MXRA5	6.59e-14	−2.3876267	3.45e-04	−1.7945193	1.56e-06	−1.1398482
MYOF	1.50e-15	−2.31380533	1.80e-05	−1.5493516	6.87e-09	−1.3488062
NMU	1.21e-07	−1.741711	7.71e-07	−3.4424442	2.18e-08	−1.0295189
NOX4	4.79e-18	−3.02767059	9.50e-05	−2.3154453	2.09e-10	−1.6264947
NPR3	2.04e-08	−1.42535705	6.59e-05	−1.8797023	1.10e-06	−1.2844418
NQO1	1.99e-06	−1.55021834	1.51e-07	−2.8756253	1.46e-10	−1.4664629
NRP2	3.65e-09	−1.00101663	7.92e-04	−1.0036763	2.27e-07	−1.0398169
NT5E	1.64e-05	−1.57562593	2.94e-03	−1.0329535	7.10e-06	−1.208268
OAS1	9.55e-07	−1.21738702	4.37e-05	−2.3434841	3.69e-08	−1.130268
OAS2	1.22e-07	−1.39078244	7.96e-04	−1.063974	3.18e-07	−1.0571731
OLR1	1.05e-13	−2.99889051	7.02e-04	−2.2324636	1.91e-04	−1.2763264
OSBPL3	5.07e-09	−1.43808519	1.23e-06	−1.8104033	3.59e-08	−1.1831684
PCDH7	9.65e-07	−1.22868649	2.91e-04	−1.4454759	8.62e-10	−1.0136969
PGM2L1	9.65e-14	−1.61020343	1.50e-04	−1.4075755	3.30e-09	−1.0538702
PKM	1.15e-12	−1.53410463	1.49e-05	−1.1332567	2.28e-09	−1.021846
PLA2R1	2.50e-08	−1.20222447	2.37e-04	−1.2000276	2.51e-07	−1.1070027
PLAC8	7.70e-04	−1.69996462	4.67e-06	−3.5791825	6.80e-08	−1.8359027
PLAT	1.12e-11	−2.53990857	4.05e-03	−1.757376	8.54e-07	−1.3462227
PLAU	2.69e-11	−2.05029247	4.78e-05	−2.2217329	2.68e-08	−1.3743673

TABLE 1 (*continued*)

	Upregulated DEGs					
	GSE15471		GSE16515		GSE28735	
	Adj *P*	Log FC	Adj *P*	Log FC	Adj *P*	Log FC
PLPP4	1.80e-11	−2.2263166	2.18e-05	−2.4051361	6.88e-12	−1.1414518
POSTN	1.94e-07	−1.33350561	1.09e-04	−2.7902679	2.53e-10	−2.6298373
PXDN	6.18e-07	−1.36897353	3.37e-03	−1.2099297	1.04e-05	−1.1653407
RAI14	2.21e-09	−1.43740669	2.98e-05	−1.2529126	1.57e-07	−1.0131847
RHBDL2	1.29e-07	−1.17563806	7.96e-05	−1.1628286	9.96e-11	−1.1258644
RUNX2	9.52e-11	−2.92838651	8.05e-04	−1.9477636	1.96e-10	−1.2121193
S100A16	1.59e-08	−1.1650921	9.73e-08	−2.110029	3.77e-10	−1.1656542
S100P	9.23e-11	−3.66658089	4.81e-09	−6.2580134	6.89e-14	−1.2260793
SCEL	4.29e-06	−1.26569808	2.44e-03	−1.1355372	6.18e-11	−1.6301907
SCNN1A	6.02e-04	−1.08886497	1.59e-03	−1.5464286	6.28e-06	−1.0022056
SDR16C5	7.10e-08	−2.31520076	2.32e-08	−4.1847444	3.80e-12	−1.5155709
SEMA3C	7.54e-09	−1.22426469	2.11e-03	−1.6503623	4.02e-04	−1.0999293
SERPINB3	3.59e-05	−1.6054987	4.16e-03	−1.8953011	6.28e-04	−1.2747167
SERPINB5	1.31e-07	−2.32054066	3.79e-08	−4.392844	1.21e-11	−2.1830693
SLC22A3	7.77e-06	−1.09781014	1.34e-04	−1.6463225	4.44e-06	−1.14787
SLC2A1	7.88e-08	−1.41478683	2.96e-10	−3.0533566	3.62e-12	−1.8381029
SLC44A4	1.94e-04	−1.27453752	3.13e-05	−2.3995452	9.50e-08	−1.2232882
SLC6A14	1.67e-09	−3.00993894	9.65e-08	−4.6265813	3.82e-12	−3.075768
SLC6A6	3.25e-14	−2.68187019	7.62e-05	−1.825323	3.86e-08	−1.2712856
SLPI	2.79e-14	−2.67459132	1.24e-08	−3.3129465	8.66e-09	−1.7899024
SRPX2	8.92e-16	−2.47287599	9.36e-04	−1.6544553	3.38e-05	−1.1052856
ST6GALNAC1	1.22e-03	−1.36196224	1.41e-04	−2.8412139	1.24e-07	−1.028552
STYK1	6.76e-06	−1.25356262	4.62e-06	−1.6294317	6.56e-13	−1.2155107
SULF1	1.31e-19	−3.68940574	1.45e-04	−2.4181396	1.52e-08	−1.9594916
SULF2	5.19e-10	−2.10614738	6.89e-04	−1.6246188	3.13e-05	−1.0889349
SULT1C2	2.42e-03	−1.3303751	3.50e-03	−1.7726936	4.11e-04	−1.0128167
SYTL2	2.17e-09	−1.66532807	3.23e-04	−1.7670993	1.40e-08	−1.0928962
TCN1	1.36e-07	−2.90090404	1.95e-04	−3.3290883	1.94e-04	−1.5896369
TFF1	1.06e-04	−2.39909674	1.28e-05	−4.6834284	4.87e-07	−1.9432884
TGFBI	7.08e-10	−1.89345065	4.10e-04	−1.6460046	1.92e-06	−1.1341551
TGM2	5.08e-09	−1.12833345	2.32e-03	−1.7831911	2.70e-06	−1.205276
THBS2	1.26e-17	−3.98457919	4.24e-04	−2.181901	2.56e-07	−1.6264449
TMC5	2.08e-04	−1.27698246	1.10e-05	−2.6388004	3.41e-07	−1.7178244
TMEM45B	1.56e-03	−1.4088581	9.04e-05	−2.1279175	5.75e-07	−1.3963273
TMPRSS4	2.04e-07	−1.9637276	1.14e-09	−4.5041304	7.48e-13	−2.2573618
TNFAIP6	7.96e-11	−2.48765791	1.06e-03	−1.5405643	1.75e-04	−1.30502
TOP2A	7.40e-06	−1.48965862	7.55e-07	−2.3640636	1.27e-07	−1.3128398
TRIM29	2.88e-10	−2.00085653	8.29e-09	−3.5036033	5.15e-11	−1.4077371
TSPAN1	1.16e-07	−1.78293915	2.62e-08	−3.6882971	1.63e-14	−2.7266844
TSPAN8	1.36e-02	−1.3032792	2.05e-07	−2.4782873	1.15e-04	−1.4074942
VCAN	5.20e-17	−3.73740193	9.41e-04	−1.9461635	1.73e-06	−1.7040513
VSIG1	1.80e-05	−1.7832075	1.95e-03	−2.200699	8.04e-08	−1.9952567
			Downregulated DEGs			
ABAT	7.74e-08	1.04113554	1.53e-04	1.7414842	5.42e-07	1.0759596
ACADL	1.67e-04	1.309813	3.68e-05	2.0830065	8.80e-07	1.6686389
ALB	2.22e-07	1.46077833	7.79e-05	1.4892635	4.12e-06	2.6310982
ANPEP	1.53e-05	2.42621752	1.10e-03	2.4850007	4.96e-06	1.8945569
AOX1	5.78e-04	1.06899195	1.86e-05	2.3824797	1.56e-09	2.0361547
AQP12B///AQP12A	3.38e-07	1.77319312	4.00e-03	1.6068264	8.50e-06	1.1688947
AQP8	7.06e-05	2.88068653	2.11e-03	3.5681394	2.55e-05	1.5447562
BACE1	1.96e-04	1.33697382	1.34e-04	1.8149867	3.46e-06	1.2745662
BNIP3	1.49e-05	1.31255588	6.37e-04	1.8414334	8.51e-05	1.093632
BTG2	5.22e-07	1.01870823	5.01e-04	1.482411	1.47e-08	1.1710536
C5	9.74e-08	1.78863462	1.65e-03	1.7982847	3.80e-06	1.1974638
CHRM3	7.26e-07	1.21565011	1.97e-03	1.0395154	1.88e-04	1.0729804
CTNND2	1.03e-04	1.1145235	8.06e-05	1.8025505	1.67e-06	1.3781816
CTRL	7.59e-04	3.00886301	5.20e-03	4.1102965	3.02e-05	2.2352664
DPP10	1.09e-07	2.10610623	1.68e-03	1.8993883	4.07e-05	1.204828
EGF	4.57e-05	2.25361836	7.83e-04	2.8202033	4.66e-05	2.0791816
EPB41L4B	3.34e-08	1.27662689	4.04e-04	1.5076869	1.36e-05	1.0014458
EPHX2	1.41e-08	1.42766027	2.27e-04	1.5900637	2.33e-09	1.309602
ERO1B	4.08e-05	1.62417116	8.13e-05	2.5162192	7.77e-09	1.9621349
ERP27	2.00e-03	2.31577382	4.01e-03	3.4721533	2.88e-05	2.5885804
F11	7.44e-07	1.32674611	8.59e-04	1.1769399	1.72e-06	2.006714
F8	1.23e-04	1.11066971	1.02e-04	1.8290128	1.47e-05	1.1382302
FAM129A	1.30e-05	1.06645494	7.63e-05	1.6379657	1.14e-05	1.0048831
FAM150B	1.18e-03	1.23501259	2.08e-05	3.2500833	7.11e-07	1.1093278
FGL1	1.35e-03	1.89436601	1.95e-03	2.8963528	2.10e-04	1.6669633
GATM	5.75e-05	1.25039334	1.30e-03	1.5289067	6.25e-04	1.6627798

(continued on next page)

TABLE 1 (*continued*)

	Upregulated DEGs					
	GSE15471		GSE16515		GSE28735	
	Adj *P*	Log FC	Adj *P*	Log FC	Adj *P*	Log FC
GNMT	1.55e-06	2.74551014	5.24e-04	2.9488702	1.89e-04	1.3901202
GP2	3.21e-02	1.92081986	1.82e-03	2.4593161	1.12e-04	2.793808
GPHA2	6.69e-07	1.86728762	7.73e-04	1.4332783	7.22e-05	1.10197
GSTA1	3.35e-04	1.87171685	3.97e-04	2.6806129	6.43e-05	1.1862356
GUCA1C	2.88e-07	1.07977556	2.27e-03	1.1651245	2.21e-05	1.321844
HOMER2	8.96e-04	1.4104841	5.11e-04	2.007722	3.37e-05	1.248792
KIAA1324	3.10e-05	1.58434185	2.54e-04	2.1736865	6.23e-07	2.0721882
KLK1	5.08e-04	2.25690227	2.94e-03	3.1178643	6.33e-05	1.9187229
LIFR	3.01e-05	1.12632478	1.46e-05	1.319066	7.71e-09	1.3452642
MCOLN3	3.64e-08	1.13701745	7.15e-05	1.1513915	1.49e-07	1.1641287
MT1G	1.95e-06	1.3722596	2.11e-04	1.8544499	7.22e-05	1.2238896
NR5A2	1.24e-03	1.28135842	6.52e-04	2.2282414	4.57e-06	2.0610724
NRG4	1.01e-06	1.60115287	2.26e-03	1.0302797	1.11e-04	1.6338384
NUCB2	5.22e-07	1.0613891	5.30e-04	1.6431302	1.22e-05	1.0996724
PAK3	2.28e-03	1.28384452	9.94e-05	1.9989158	1.89e-06	1.4388473
PDIA2	4.07e-05	2.61613826	2.08e-03	3.7840517	9.44e-06	2.1084087
PDK4	1.89e-05	1.37573077	1.56e-06	2.4030511	6.18e-07	1.61166
PM20D1	2.63e-07	2.41556837	3.83e-03	1.8976107	7.82e-05	1.380062
PNLIPRP1	3.32e-02	2.04233634	2.38e-03	4.0693577	3.86e-05	3.0266571
RBPJL	2.13e-06	2.35782027	1.36e-03	2.9782084	1.74e-05	1.7077773
RGN	1.21e-04	1.09262047	1.32e-04	2.1504185	3.81e-07	1.2929591
SERPINI2	1.63e-03	2.97325268	1.78e-03	4.2512033	2.38e-05	2.4767376
SLC16A10	1.50e-06	1.92460149	2.10e-05	1.9189034	4.74e-04	1.0443833
SLC1A2	1.46e-06	1.01926645	8.71e-04	1.6966492	9.13e-05	1.0052447
SLC39A5	1.85e-08	1.59792695	1.02e-03	1.5697093	2.57e-05	1.2896791
SLC43A1	3.32e-06	1.66833588	6.63e-04	1.9614561	1.22e-05	1.1801271
TMED6	9.89e-05	2.76897653	6.43e-04	3.5223984	2.09e-06	1.8966689
TRHDE	2.83e-08	2.25612973	2.00e-04	2.4896933	1.18e-05	1.680468

If the |Log FC| > 1, and Adj $P < .05$, it means that the gene has more than 10-fold change between pancreatic cancer and normal tissue, and the difference is statistically significant. The adjusted *P* values are listed in the Adj *P* value column of the results table. The Benjamini & Hochberg false discovery rate method is selected by default in GEO as it is the most commonly used adjustment for microarray data and provides a good balance between discovery of statistically significant genes and limitation of false positives.

sure the knockout effect. Sequencing was done by Eurofins, and all selected clones were sequenced at least five times.

Proliferation Assay

Cell counting was used to analyze the proliferation ability between ECT2 knockout clones and negative control clone. Cells were plated as 3×10^3 cells per well in grown medium on 96-well black plates (Costar, #3603) for 4 days. After 24, 48, and 72 hours of proliferation, cells were stained with NucBlue Live Cell Stain ReadyProbes reagent (Invitrogen, R37605) and imaged in 38 fields for each well by Evos FL Auto 2 imaging system (Invitrogen, AMAFD2000). Images were counted by HCS studio cell analysis software (Thermo, SX000041A). All experiments were done in duplicate and repeated at least three times.

Migration Assay

FluoroBlok Insert system (Corning, REF351152) was used to analyze the migration ability between ECT2 knockout clones and negative control clone. After incubation with medium without FCS for 24 hours cells were plated as 25,000 cells per well in FluoroBlokTM Insert, and put FluoroBlokTM Insert into Multi-well 24 Well (Corning, REF353504). The medium in the upper compartment was without FCS, in the lower compartment the growth medium contained 20% FCS. After 16 hours of migration in a cell culture incubator, the NucSpot Live 488 Nuclear Stain (Biotium, Cat40081) was used, and the cells attached on center of the membrane were imaged in random four fields for each well by Evos FL Auto 2 imaging system (Invitrogen, AMAFD2000).The positive point in all images was manually counted.

Statistical Analysis

Statistical analysis was performed with GraphPad Version 7 and Microsoft Excel Version 2017. For cell culture experiments, *t* test was used. For interpretation of differences, a *P* value $< .05$ was considered as statistically significant.

Results

Identification of DEGs in Gene Expression Microarrays

We identified 1647, 1693, and 407 DEGs in pancreatic cancer tissue compared to normal tissue in the GSE15471, GSE16515, and GSE28735 datasets, respectively. A total of 236 genes were considered DEG in all the 3 datasets (Figure 1 and Table 1, see Materials and Methods). In particular, 182 genes were upregulated and 54 genes were downregulated.

Functional and Pathway Enrichment Analysis

DAVID was used to analyze the functions and pathways (see Materials and Methods) of identified DEGs. DEGs were mainly involved in biological processes associated integrin-mediated signaling pathway, proteolysis, and collagen catabolic process. Moreover, seven KEGG pathways were overrepresented among upregulated genes, including ECM-receptor interaction, focal adhesion, and PI3K-Akt signaling pathway (Table 2).

PPI Network Construction and Modules Selection

The PPI network (see Materials and Methods) included 182 upregulated (176 nodes and 282 edges) and 54 downregulated (52 nodes and 10 edges) DEGs (Figure 2*A*). A total of 12 genes, including

Table 2. Functional and Pathway Enrichment Analysis of Upregulated and Downregulated Genes in Pancreatic Cancer with the DEGs in the Three mRNA Expression Profiling Datasets

Term	Description	Count	*P* Value
Upregulated			
GO:0030198	integrin-mediated signaling pathway	21	1.05E-14
GO:0030574	collagen catabolic process	14	6.69E-14
KEGG:hsa04512	ECM-receptor interaction	13	1.88E-10
GO:0004222	metalloendopeptidase activity	12	1.65E-08
GO:0030199	collagen fibril organization	8	1.17E-07
KEGG:hsa04510	Focal adhesion	14	4.69E-07
KEGG:hsa05146	Amoebiasis	10	2.82E-06
GO:0005201	extracellular matrix structural constituent	8	4.49E-06
GO:0004252	serine-type endopeptidase activity	13	9.59E-06
KEGG:hsa04151	PI3K-Akt signaling pathway	15	2.96E-05
GO:0005581	collagen trimer	8	3.05E-05
GO:0031581	hemidesmosome assembly	4	2.13E-04
KEGG:hsa04974	protein digestion and absorption	7	4.74E-04
GO:0007229	integrin-mediated signaling pathway	7	5.24E-04
GO:0005788	endoplasmic reticulum lumen	9	5.65E-04
GO:0006508	proteolysis	15	6.11E-04
GO:0007160	cell-matrix adhesion	6	0.00226
KEGG:hsa05222	small cell lung cancer	6	0.002763
KEGG:hsa05200	Pathways in cancer	12	0.004792
GO:0043588	skin development	4	0.004925
GO:0048333	mesodermal cell differentiation	3	0.005338
Downregulated			
GO:0003756	protein disulfide isomerase activity	3	0.001837

Table 3. Significant Prognostic Value of Hub Genes and Screening Out DEGs in Pancreatic Cancer Patients

10% vs 90%					
Gene name	COMP	FN1	ITGB4	COL8A1	COL10A1
Log-rank *P* value	.0193	.0301	.000194	.00444	.00158
Gene name	COL5A2	ITGA2	ITGA3	THBS2	COL3A1
Log-rank *P* value	.00416	.0309	.0252	.0207	.00386
Gene name	ECT2	NRP2	TGFBI		
Log-rank *P* value	.00124	.0177	.0199		
20% vs 80%					
Gene name	ITGB4	COL11A1	ITGA2	ITGA3	THBS2
Log-rank *P* value	.000842	.0241	.0152	.000484	.00866
Gene name	ECT2	NRP2	TGFBI		
Log-rank *P* value	.00484	.00801	.0448		
40% vs 60%					
Gene name	ITGB4	COL11A1	ITGA2	ITGA3	
Log-rank *P* value	.00836	.0113	2.91e-06	6.21e-05	
Gene name	ECT2	NRP2	TGFBI		
Log-rank *P* value	.000851	.059	.0343		

THBS2and ITGA3, have more than 10 interaction partners (Figure 2*B*) and are potential hub genes. A significant module was observed in the PPI network of DEGs (Figure 2*B*). Overall survival analysis of the hub genes (see Materials and Methods) showed that the expression level of most of them (10/12) is strongly associated with the overall survival in pancreatic adenocarcinoma. In particular, low expression levels (bottom 10%) are associated with poor survival, while high expression levels (top 90%) are associated with improved survival (Table 3, 10% vs 90% part). However, the effect decreases when patients are split into the bottom 20% and upper 80% and into the bottom 40% and upper 60% according to their expression values for the corresponding genes, with 5/12 and 4/12 hub genes showing a significant correlation with the overall survival, respectively (Table 3, 20% vs 80% and 40% vs 60% part). (See Fig. 3.)

MiRNA-DEG Pairs

We identified 21 DEMs in pancreatic cancer tissue compared to normal tissue in the GSE41372 dataset. In particular, 19 miRNAs were upregulated and 2 were downregulated (Table 4). Using miRecords (see Materials and Methods), we predicted 718 gene targets for these DEMs. Specifically, four predicted DEM targets were DEGs: NRP2 was among the predicted gene targets of miR27a, and miR331-3p, ECT2, NR5A2, and TGFBI were among the predicted gene targets of miR302c, miR27a, and miR21, respectively.

Overall Survival Analysis

We used OncoLnc to conduct overall survival analysis of ECT2, NR5A2, NRP2, and TGFBI in pancreatic cancer. We found that

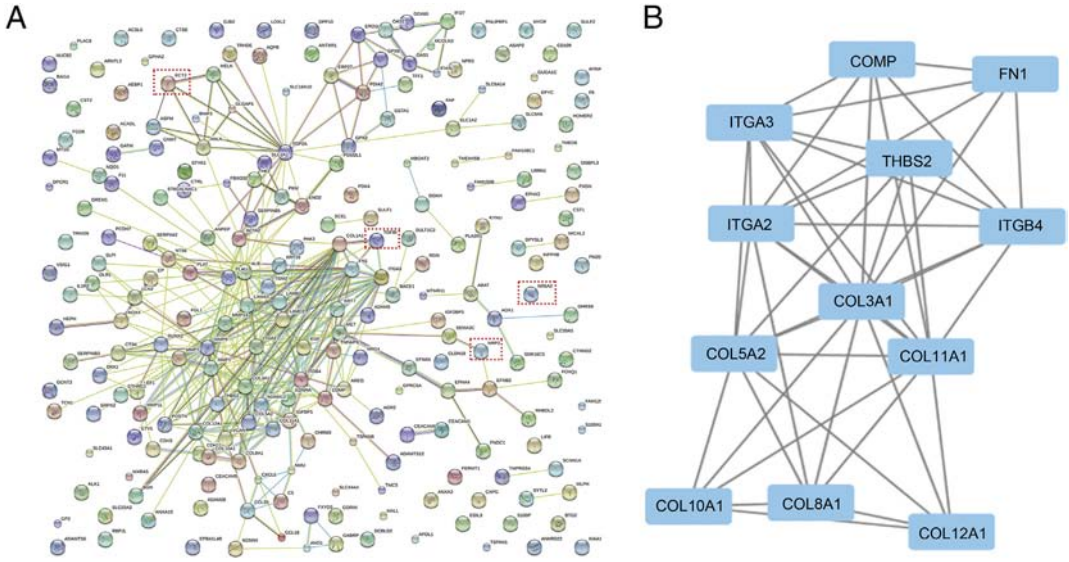

Figure 2. PPI network and a significant module. (A) PPI network of total DEGs in the three mRNA expression profiling datasets. (B) A significant module selected from PPI network. All the genes are upregulated genes. The line represents interaction relationship between nodes.

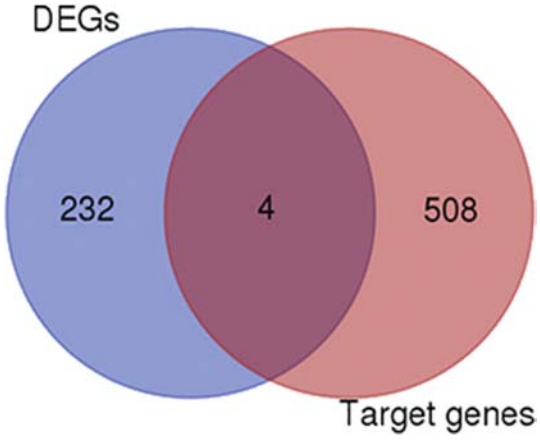

Figure 3. Identification of DEGs and paired miRNAs in the three mRNA expression and one miRNA expression profiling datasets. We found four specially DEGs and their miRNA, including ECT2-miR302c, NR5A2-miR27a, NRP2-miR27a, and miR331-3p, TGFBI-miR21.

high mRNA expression of ECT2, NRP2, or TGFBI was associated with worse overall survival (log-rank *P* value = .001, .02, and .02, respectively; Figure 4, *A-D* and Table 3). We also analyzed the predicted DEM regulators of the four DEGs and found that high expression of miR27a and miR21 was associated with worse overall survival (log-rank *P* values = .001 and .002, respectively; Figure 4, *E* and *F*). There was no significant association between miR302C expression and overall survival (data not shown). Then, we changed the percentage from 10% vs 90% to 20% vs 80%; the results also showed that high expression of ECT2, NRP2, or TGFBI was associated with worse overall survival (Table 3). Finally, we also investigated associations between the DEGs and other kinds of cancer, including breast, lung, colorectal, and prostate cancer (Table 5).

Expression of DEGs in Different Organs

We used " The Human Protein Atlas " to perform the basic expression level of DEGs in different human organs. We found that the basic expression of ECT2, NRP2, and TGFBI was at lower level than other organs with HPA dataset, GTEx dataset, and FANTOM5 dataset (Figure 5*A*, GTEx and FANTOM% not shown). We also analyzed the basic expression of DEGs in pancreas and cancer tissues with TCGA dataset. Those results showed that the expression of ECT2 and NRP2 was significant higher in pancreatic cancer tissues, but there was no significant difference in expression on TGFBI (Figure 5*B*). Furthermore, we found that NRP2 expression in pancreatic cancer is a big difference.

Expression of DEGs in Normal Pancreas and Pancreatic Cancer Cell Lines

For further research of the different expression of DEGs in pancreatic cancer, we detected the protein expression between normal pancreas HDPE cell and different pancreatic cancer cell lines by Western blot. Those results showed that the protein expression of ECT2 in pancreatic cancer cell lines was higher than that in normal pancreas cell line. The expression of NRP2 was higher in some kinds of pancreatic cancer cell lines, such as ASPC1, PaCaDD119, PaCaDD137, and PaCaDD159, than normal pancreas cell line. There was higher expression level of TGFBI in normal pancreas cell line (Figure 6*A*). The q-PCR showed the same results with Western blot (Figure 6*B, C,* D). ECT2 was completely overexpressed in pancreatic cancer cell lines. NRP2 and TGFBI were partly overexpressed and obviously not overexpressed, respectively, in pancreatic cancer cell lines.

Table 4. DEMs in Pancreatic Cancer Screened Out from miRNA Expression Microarray GSE41372 and Their Target Genes Predicted by miRecords

miRNA	Adj.P	logFC	Target Genes
hsa-miR-630	0.002038	−4.21846	NA
hsa-miR-302c	0.002434	−1.37368	E2F7, PARP8, NEUROD6, SLC22A23, CFL2, DMTF1, TNFAIP1, ZNFX1, TSHZ3, DCUN1D1
hsa-miR-337-3p	0.003922	1.307959	NA
hsa-miR-190b	0.005768	1.369034	NA
hsa-miR-140-3p	0.003638	1.504247	NA
hsa-miR-331-3p	0.003497	1.830589	B4GALT2, ZNF513, RIC8B, BAIAP2, CPSF2, CAMK2A, SNX17, PHC2, DAG1, NRP2
hsa-miR-484	0.002038	1.835517	NA
hsa-miR-490-3p	0.001403	1.888625	NA
hsa-miR-342-3p	0.002434	2.136132	PPP3R1, ZAK, BTN2A1, MRFAP1, ZIC4, RSBN1, FAM53C, PDGFRA, FUT8, UBE2D2
hsa-miR-221	0.000713	2.181648	CDKN1B, ATXN1, TMCC1, NSMCE4A, GOLSYN, EIF5A2, DCUN1D1, DMRT3, C12orf30, MIER3
hsa-miR-197	0.001103	2.192276	NA
hsa-miR-1975	0.003424	2.291544	NA
hsa-miR-125a-5p	0.002574	2.483418	MCL1, SLITRK6, OSBPL9, ELOVL6, NIN, ALPK3, CGN, GTPBP2, CCNJ, SYVN1
hsa-miR-142-5p	0.003922	2.625738	BTBD7, RAB6B, FLJ10357, LRP1B, TRIM36, ALS2, EGLN3, CHD9, WDR26, SCOC
hsa-miR-135b	3.37E-05	2.819987	TSEN54, GGNBP2, C6orf106, NUCKS1, TMEM168, PELI2, LZTS1, NUDT4, HOXA10, ELOVL2
hsa-miR-10a	0.001103	2.841119	TBX5, NARG1, HOXA3, USP46, BACH2, RAP2A, SLC38A2, ANKFY1, NCOA6, BAZ2B
hsa-miR-223	0.002038	2.930734	NFIA, FBXO8, STK39, SACS, RBM16, PDS5B, PHF20L1, CRIM1, FBXW7, SLC8A1
hsa-miR-21	0.001978	2.992536	RP2, JAG1, SOX5, LEMD3, KIAA1012, BAHD1, ADNP, ASPN, CHD7, PELI1
hsa-miR-145	0.001133	3.244704	MDFIC, CACHD1, EPB41L5, SEMA6A, NUFIP2, SRGAP1, RIN2, CDC37L1, KIF21A, INOC1
hsa-miR-199a-5p	0.007061	3.264147	ATXN7, C11orf9, CELSR1, RAB10, CCNJ, CCNL1, SLC24A3, ZNF512B, ALS2, CCDC43
hsa-miR-27a	0.003424	3.636233	TMCC1, NXT2, HOXA10, DLL4, CCNJ, ANK1, SEMA6A, GPAM, OTX2, TEAD1

CRISPR/Cas9 Gene Editing

We detected ECT2 function to verify the data mining results. From the basic expression of different pancreatic cancer cell lines and normal pancreas cell line, we found that there was higher expression of ECT2 in MiaPaCa2 cell line. Then, we used Crispr Cas9 gene editing system to knockout ECT2 in MiaPaCa2 cells (Figure 7*A*). We detected the proliferation ability with ECT2 knocked out cells, negative control cells, and wild-type cells. Those results showed that

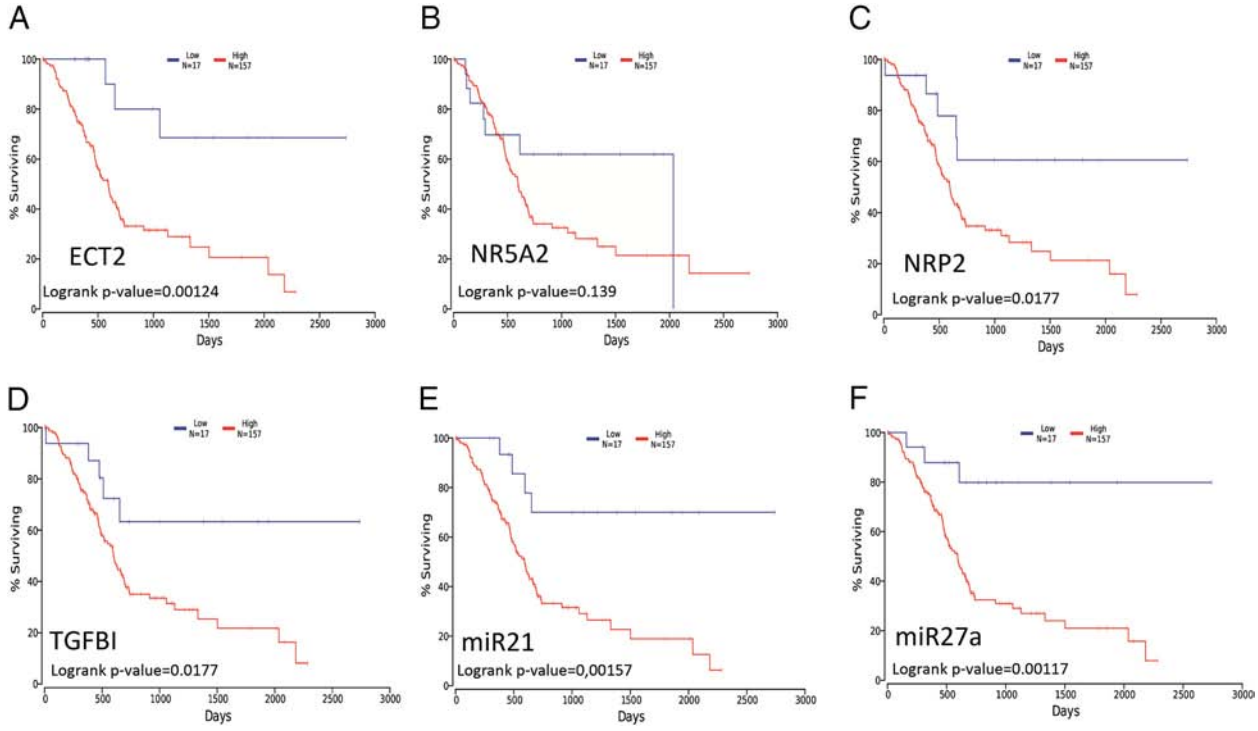

Figure 4. Prognostic value of four DEGs and their miRNA in pancreatic cancer patients. Prognostic value of (A) ETC2 (log-rank *P* value = .00124), (B) NR5A2 (log-rank *P* value = .139), (C) NRP2 (log-rank *P* value = .0177), (D) TGFBI (log-rank *P* value = .0199), (E) miR21 (log-rank *P* value = .00157), and (F) miR27a (log-rank *P* value = .00117).

ECT2 knocked out cells grew slower than negative control and wild-type cells (Figure 7*B*). Furthermore, we also detected the migration ability with ECT2 knocked out cells. Those results showed that the migration ability of ECT2 knocked out cells was lower than negative control and wild-type cells (Figure 7, *C* and *D*).

Discussion

Pancreatic cancer is a nearly universally fatal disease and is one of the few cancer types that continue to increase in incidence [33]. It is expected to become the second leading cause of cancer-related deaths in the United States in the next few years. Peak incidence of pancreatic cancer has been linked to few predisposing factors, including cigarette smoking, red meat, obesity, and heavy alcohol consumption along with pancreatic disease [34–36]. Because of its aggressive behavior and frequently late diagnosis, research aiming at early diagnosis of pancreatic cancer or its precursors is crucial. Molecular biomarkers play an important role in early diagnosis, and the rapid development of high-throughput technologies has resulted in an increasing number of biomarkers being screened for disease progression [37,38]. Biomarkers enable the identification of genes, miRNAs, LncRNAs, and so on for early diagnosis, treatment, and prognosis of the disease, including pancreatic cancer. In particular, microarray and follow-up experiments performed in our laboratory over the last few years [39,40] have shown that we can identify biomarkers and key genes in pancreatic cancer [39,41].

In this study, we used three mRNA and one miRNA expression microarray datasets to identify biomarkers in pancreatic cancer. The four expression microarrays correspond to two different platforms, making the screen result more robust. We performed a comprehensive analysis of the DEMs, including functional and pathway enrichment analysis, and PPI analysis. Next, we screened the DEGs among the putative targets of the DEMs. Compared to previous studies [15,42,43], the samples included were more comprehensive and random. We identified a total of 236 DEGs among the three mRNA expression microarray datasets, consisting of 182 up-and 54 downregulated genes. Upregulated DEGs were mainly associated with the integrin-mediated signaling pathway, proteolysis, and the PI3K-Akt signaling pathway, which have been proved to have a close relationship with pancreatic cancer [44]. Twelve of the 236 DEGs were highly connected in the PPI network and were in the core of the PPI network. Such hub genes are usually the focus of microarray-based biomarker research. Indeed, an overall survival analysis with the clinical data from TCGA showed the expected trend, with 10 of these genes being strongly associated with overall survival in pancreatic adenocarcinoma. However, the correlation between increased overall survival and low expression levels is only strong for the bottom 10%, and the number of hub genes displaying a significant correlation decreases to 5 or 4 when then 20th and 40th percentiles are considered. In addition, we identified 21 DEMs and their more than 500 predicted target genes. In order to improve the generalizability and robustness of the predictions, DEM target predictions were

Table 5. Prognostic Value of Four DEGs in Other Kinds of Cancer Patients

Gene/Cancer Name	ECT2	NR5A2	NRP2	TGFBI
Breast cancer	0.956	0.254	0.57	0.869
Gastric cancer	0.983	0.794	0.091	0.00395
Lung cancer	0.0433	0.965	0.975	0.862
Ovarian cancer	0.193	0.622	0.992	0.611
Liver cancer	0.00295	0.614	0.00763	0.457

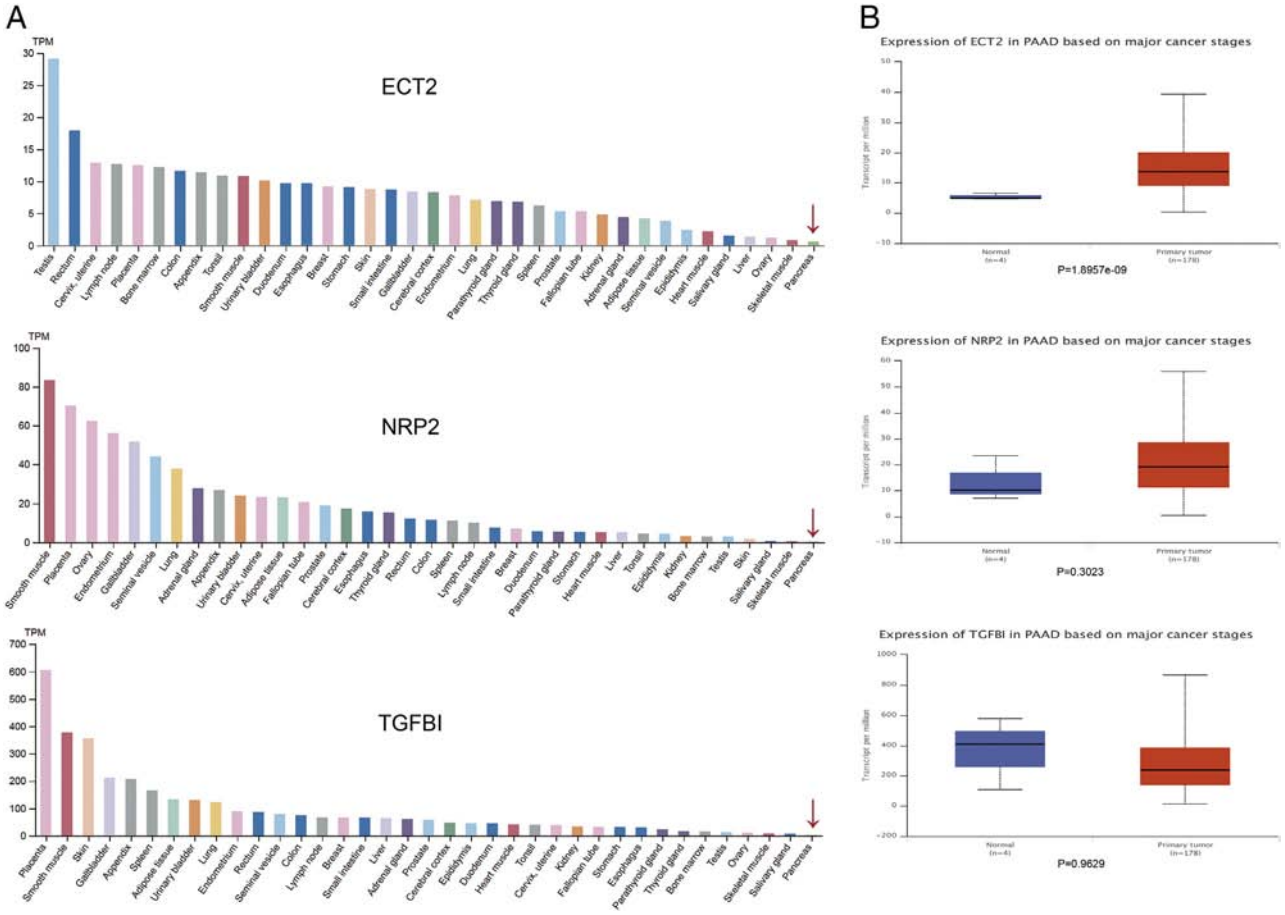

Figure 5. The basic expression of DEGs in different organs and cancer. The basic expression of DEGs in pancreas stood lower level in 37 kinds of organs (A). The expressions of ECT2 and NRP2 were significant higher in pancreatic cancer tissues (B).

obtained with an ensemble approach [30]. Four DEM targets were also DEGs: ECT2 (miR302c), NR5A2 (miR27a), NRP2 (miR27a and miR331-3p), and TGFBI (miR21). All four DEGs were upregulated in pancreatic cancer tissue. miRNA including miR27a, miR331-3p, and miR21 were upregulated; miR302c was downregulated. NR5A2 has been reported to be upregulated in pancreatic cancer [45]; ECT2, NRP2, and TGFBI are novel candidates. Overall survival analysis of these genes showed that upregulation of ECT2, NRP2, or TGFBI is significantly correlated with poor survival of pancreatic cancer patients. Interestingly, 7 patients had low expression levels for ECT2, NRP2, and TGFBI, and 13 patients had low expression levels for 2 of these 3 genes. However, this finding warrants further investigation.

ECT2 locates at 3q26.31, is a BRCT-containing guanidine exchange factor for Rho GTPases, and was found to be a responder to DNA damage [46]. It controls cell division and exerts oncogenic functions in multiple cancers [47,48]. Patients with high expression of ECT2 also have poor overall survivals in lung (log-rank P value = .04) and liver (log-rank P value = .003) cancer. Additionally, ECT2 has been reported to play an important role in the Wingless/Wnt and KRAS signaling pathways [49,50]. The KRAS is a key signaling pathway in pancreatic cancer. Typical alterations in the molecular signaling include mutations in KRAS in 95% of pancreatic cancer [41,51]. Consistent with our results, previous studies have also shown that ECT2 is an oncogene which is overexpressed in pancreatic tumor tissues [52]. However, the oncogenic mechanism for pancreatic cancer has rarely been explored. NRP2 is located at 2q33.3; is a nontyrosine kinase receptor frequently overexpressed in various malignancies; and may play a role in cardiovascular development, axon guidance, and tumorigenesis [53]. Some studies have shown that it is required for maintaining endocytic activity in cancer cells, which supports their oncogenic activities and confers drug resistance [54]. Further, it has been suggested that NRP2 works its biological function via the GSK3β and VEGFC/VEGFR3 signaling pathway [55,56], and GSK3β plays a key role in resistance to pancreatic cancer therapy [57]. We performed overall survival analysis of NRP2 in some common tumors and found that upregulated NRP2 is significantly correlated with poor overall survival of liver (log-rank P value = .008) tumor patients. In our study, NRP2 we could not confirm a significant correlation of NRP2 expression and survival in breast and gastric cancer, but other studies have shown a function in breast and gastric tumor, proving that it is an important gene in solid tumors [58,59]. However, there is no study focused on NRP2 function in pancreatic cancer. Finally, TGFBI, also known as βig-H3, is a protein inducible by TGFβ1 and secreted by many cell types [60]. Furthermore, TGFBI is an important component of the Wnt signaling pathway [61]. It is located at 5q31.1. In our study, the patients with upregulated TGFBI have poor survival rate in gastric (log-rank P value = .004) and pancreatic (log-rank P value = 2.0×10^{-2}) cancer. TGFBI has been studied in the context of many

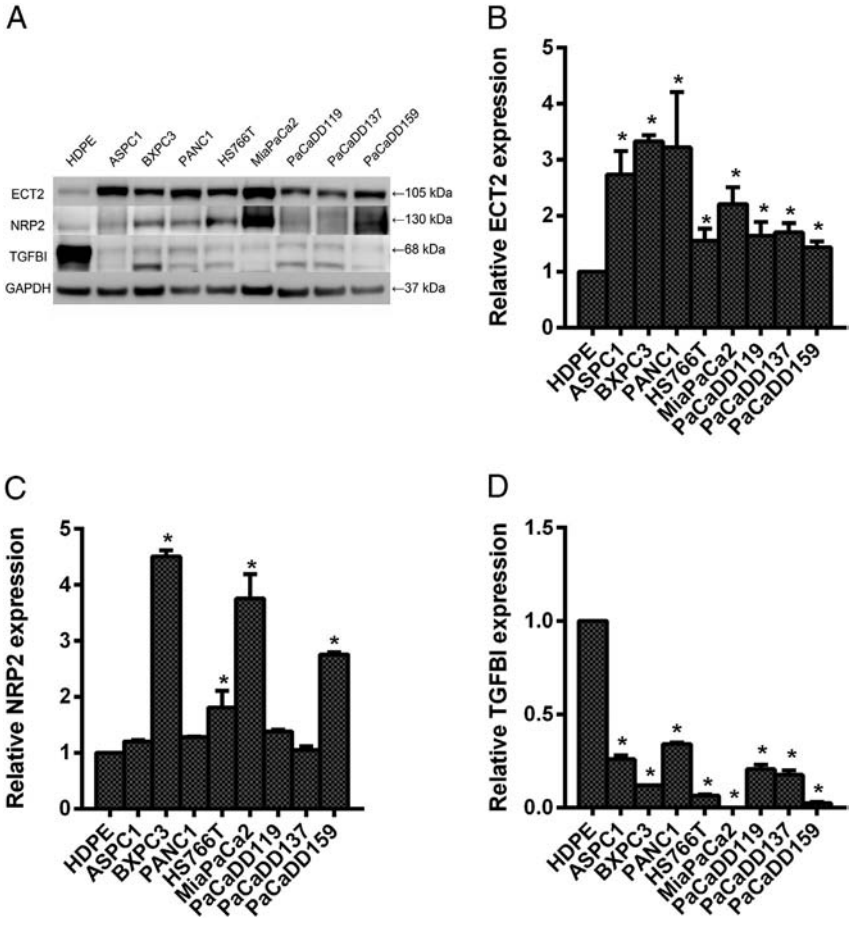

Figure 6. The basic expression of DEGs in normal pancreas and pancreatic cancer cell lines. The protein expression of DEGs in normal pancreas and pancreatic cancer cell lines (A). The mRNA expression of DEGs in normal pancreas and pancreatic cancer cell lines (B, C, D). *P value < .05.

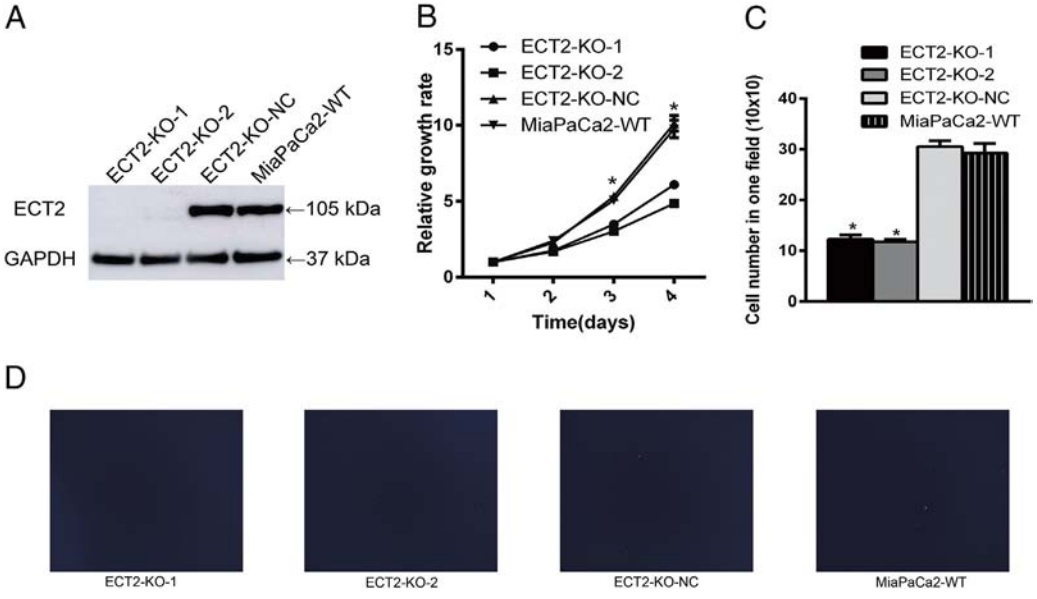

Figure 7. Knockout of ECT2 decreased proliferation and migration ability in MiaPaCa2 cells. Knockout of ECT2 by Crispr Cas9 gene editing system inhibited protein expression of ECT2 in MiaPaCa2 cells (A). ECT2 knocked out cells grew slower than control groups (B). ECT2 knocked out cells migration slower than control groups (C and D). *P value < .05.

different diseases, but no study has revealed its function and mechanism in pancreatic cancer. Interestingly, all ECT2, NRP2, and TGFß1 are involved in the Wnt signaling pathway, which has been reported to be an important regulated part and potential treatment target in pancreatic cancer in multiple studies. These observations support our hypothesis that ECT2, NRP2, and TGFBI are potential regulated components of pancreatic cancer and that there may be more interactions among them. Together with NR5A2, these four genes grant further *in vivo* and *in vitro* study.

Among the 21 DEMs in pancreatic cancer, we identified 19 upregulated and 2 downregulated miRNAs. miR27a was the strongest upregulated miRNA, and miR630 was the strongest downregulated miRNA. Some studies have reported that miR27a is a cooperative repressor of a network of tumor suppressor genes, and inhibition of miR27a has been shown to have synergistic effects in reducing proliferation of PDAC cells in culture and growth of xenograft tumors in mice [22]. NR5A2 and NRP2 are the predicted targets of miR27a, and ECT2, NR5A2, NRP2, and TGFBI were DEGs in the three mRNA expression datasets. miR21, miR302c, and miR331-3p potentially play a role in pancreatic cancer.

We also checked the basic expression of DEGs in different organ. We found that the basic expression of ECT2, NRP2, and TGFBI was at a lower level than other organs with HPA dataset, GTEx dataset, and FANTOM5 dataset. In HPA dataset, those 3 DEGs were the last one of 37 organs. However, in the comparison of expression between pancreas and pancreatic cancers from TCGA, we can that found ECT2 and NRP2 were statistically significantly higher in cancer tissues. It predicted that the higher expression of ECT2 and NRP2 may play a role in tumorigenicity of pancreatic cancer.

For further verification of above data-mining results, we used basic biology experiment to detect the basic expression of ECT2, NRP2, and TGFBI in normal pancreas cell line and pancreatic cancer cell lines. Those results proved that ECT2 and NRP2 had higher expression level in pancreatic cancer. However, there was higher expression level of TGFBI in normal pancreas cell line. Globally expressed ECT2 was associated with worse overall survival stably. Mixed expressed NRP2 was associated with worse overall survival based on the percentiles of expression values and cancer kinds. Outlier expressed TGFBI was associated with worse overall survival occasionally (Tables 3 and 5). We think ECT2 and NRP2 may play an important role in pancreatic cancer.

Furthermore, we also did gene function analysis by experiment. We made MiaPaCa2 ECT2 knockout stable cell lines to verify the above results with Crispr Cas9 system. As those results showed, knockout of ECT2 decreased the proliferation and migration ability of MiaPaCa2 cells. It predicted that ECT2 was an important gene in pancreatic cancer. This is in line with expectations based on above results.

This study is a next step in identifying relevant biomarkers for early diagnosis and progression of pancreatic cancer. In this study, we combined high-throughput mRNA and miRNA expression datasets with functional and regulatory network analyses to screen for biomarkers. miR21, miR27a, miR302c, and miR331-3p and their predicted targets genes ECT2, NRP2, and TGFBI were selected as promising candidates. Then, we detected the basic expression level of DEGs in various organ tissues and different pancreatic cancer with data mining and experiment methods. Those showed that ECT2 and NRP2 were in line with data mining results. We also used Cripsr Cas9 gene editing system to knockout ECT2 and proved its important function in pancreatic cancer. Meanwhile, we will continue to research ECT2 and NRP2 functions and mechanisms in pancreatic cancer and assess their clinical application prospects. We believe that ECT2 and NRP2 can play as potential biomarker in pancreatic cancer patients, and they may be potential target therapy site with Crispr Cas9 gene editing system for pancreatic cancer.

Funding

B. L. is funded by the China Scholarship Council (CSC) scholarship (No. 201406210072).

Availability of Data and Materials

All source data are available on the appropriate Web sites.

Author's Contributions

Conceptualization: B. L., C. P.
Data curation: B. L.
Formal analysis: B. L.
Funding acquisition: B. L C. P., R. G.
Supervision: C. P.
Writing, original draft: B. L.
Writing, review & editing: B. L., H. Y., L. T., A. D., R. G., C. P., G. W.
All authors participated in the process of revision and finalizing the manuscript. All authors read and approved the final manuscript.

Competing Interests

All authors declare that they have no competing interest.

Consent for Publication

Not applicable.

Ethics Approval and Consent to Participate

Not applicable.

Previous Presentation as Congress Abstract

Not applicable.

Acknowledgements

We like to thank all the scientists who were able to put their software and data online. Without the efforts of the research community, this study would have been impossible.

References

[1] New M, Van Acker T, Long JS, Sakamaki JI, Ryan KM, and Tooze SA (2017). Molecular pathways controlling autophagy in pancreatic Cancer. *Front Oncol* **7** 28.
[2] Siegel RL, Miller KD, and Jemal A (2016). Cancer statistics, 2016. *CA Cancer J Clin* **66**, 7–30.
[3] Chen W, Zheng R, Baade PD, Zhang S, Zeng H, Bray F, Jemal A, Yu XQ, and He J (2016). Cancer statistics in China, 2015. *CA Cancer J Clin* **66**, 115–132.
[4] De Angelis R, Sant M, Coleman MP, Francisci S, Baili P, Pierannunzio D, Trama A, Visser O, Brenner H, and Ardanaz E, et al (2014). Cancer survival in Europe 1999-2007 by country and age: results of EUROCARE–5-a population-based study. *Lancet Oncol* **15**, 23–34.
[5] Lianos GD, Christodoulou DK, Katsanos KH, Katsios C, and Glantzounis GK (2017). Minimally invasive surgical approaches for pancreatic adenocarcinoma: recent trends. *Int J Gastrointest Cancer***48**, 129–134.
[6] Griffin JF, Poruk KE, and Wolfgang CL (2015). Pancreatic cancer surgery: past, present, and future. *Chin J Cancer Res* **27**, 332–348.
[7] Zhou B, Xu JW, Cheng YG, Gao JY, Hu SY, Wang L, and Zhan HX (2017). Early detection of pancreatic cancer: Where are we now and where are we going? *Int J Cancer***141**, 231–241.

[8] Halbrook CJ and Lyssiotis CA (2017). Employing metabolism to improve the diagnosis and treatment of pancreatic cancer. *Cancer Cell* **31**, 5–19.
[9] Chang JC and Kundranda M (2017). Novel diagnostic and predictive biomarkers in pancreatic adenocarcinoma. *Int J Mol Sci* **18**, E667.
[10] Stojkovic Lalosevic M, Stankovic S, Stojkovic M, Markovic V, Dimitrijevic I, Lalosevic J, Petrovic J, Brankovic M, Pavlovic Markovic A, and Krivokapic Z (2017). Can preoperative CEA and CA19-9 serum concentrations suggest metastatic disease in colorectal cancer patients? *Hell J Nucl Med***20**, 41–45.
[11] Zhou G, Liu X, Wang X, Jin D, Chen Y, Li G, Li C, Fu D, Xu W, and Wang X (2017). Combination of preoperative CEA and CA19-9 improves prediction outcomes in patients with resectable pancreatic adenocarcinoma: results from a large follow-up cohort. *Onco Targets Ther* **10**, 1199–1206.
[12] Distler M, Pilarsky E, Kersting S, and Grutzmann R (2013). Preoperative CEA and CA 19-9 are prognostic markers for survival after curative resection for ductal adenocarcinoma of the pancreas - a retrospective tumor marker prognostic study. *Int J Surg* **11**, 1067–1072.
[13] Zhu L, Xue HD, Liu W, Wang X, Sui X, Wang Q, Zhang D, Li P, and Jin ZY (2017). Enhancing pancreatic mass with normal serum CA19-9: key MDCT features to characterize pancreatic neuroendocrine tumours from its mimics. *Radiol Med* **122**, 337–344.
[14] Swords DS, Firpo MA, Scaife CL, and Mulvihill SJ (2016). Biomarkers in pancreatic adenocarcinoma: current perspectives. *Onco Targets Ther* **9**, 7459–7467.
[15] Grutzmann R, Boriss H, Ammerpohl O, Luttges J, Kalthoff H, Schackert HK, Kloppel G, Saeger HD, and Pilarsky C (2005). Meta-analysis of microarray data on pancreatic cancer defines a set of commonly dysregulated genes. *Oncogene* **24**, 5079–5088.
[16] Krizkova S, Kepinska M, Emri G, Rodrigo MA, Tmejova K, Nerudova D, Kizek R, and Adam V (2016). Microarray analysis of metallothioneins in human diseases—a review. *J Pharm Biomed Anal* **117**, 464–473.
[17] Stewart JP, Richman S, Maughan T, Lawler M, Dunne PD, and Salto-Tellez M (2017). Standardising RNA profiling based biomarker application in cancer-The need for robust control of technical variables. *Biochim Biophys Acta* **1868**, 258–272.
[18] Badea L, Herlea V, Dima SO, Dumitrascu T, and Popescu I (2008). Combined gene expression analysis of whole-tissue and microdissected pancreatic ductal adenocarcinoma identifies genes specifically overexpressed in tumor epithelia. *Hepato-Gastroenterology* **55**, 2016–2027.
[19] Pei H, Li L, Fridley BL, Jenkins GD, Kalari KR, Lingle W, Petersen G, Lou Z, and Wang L (2009). FKBP51 affects cancer cell response to chemotherapy by negatively regulating Akt. *Cancer Cell* **16**, 259–266.
[20] Zhang G, He P, Tan H, Budhu A, Gaedcke J, Ghadimi BM, Ried T, Yfantis HG, Lee DH, and Maitra A, et al (2013). Integration of metabolomics and transcriptomics revealed a fatty acid network exerting growth inhibitory effects in human pancreatic cancer. *Clin Cancer Res* **19**, 4983–4993.
[21] Zhang G, Schetter A, He P, Funamizu N, Gaedcke J, Ghadimi BM, Ried T, Hassan R, Yfantis HG, and Lee DH, et al (2012). DPEP1 inhibits tumor cell invasiveness, enhances chemosensitivity and predicts clinical outcome in pancreatic ductal adenocarcinoma. *PLoS One* **7**, e31507.
[22] Frampton AE, Castellano L, Colombo T, Giovannetti E, Krell J, Jacob J, Pellegrino L, Roca-Alonso L, Funel N, and Gall TM, et al (2014). MicroRNAs cooperatively inhibit a network of tumor suppressor genes to promote pancreatic tumor growth and progression. *Gastroenterology* **146**, 268–277 e218.
[23] Edgar R, Domrachev M, and Lash AE (2002). Gene Expression Omnibus: NCBI gene expression and hybridization array data repository. *Nucleic Acids Res* **30**, 207–210.
[24] Gan Z, Wang J, Salomonis N, Stowe JC, Haddad GG, McCulloch AD, Altintas I, and Zambon AC (2014). MAAMD: a workflow to standardize meta-analyses and comparison of affymetrix microarray data. *BMC Bioinformatics* **15**, 69.
[25] Vilming Elgaaen B, Olstad OK, Haug KB, Brusletto B, Sandvik L, Staff AC, Gautvik KM, and Davidson B (2014). Enhancing pancreatic mass with normal serum CA19-9: key MDCT features to characterize pancreatic neuroendocrine tumours from its mimics. *BMC Cancer* **14**, 80.
[26] Benjamini Y and Hochberg Y (1995). Controlling the false discovery rate — a practical and powerful approach to multiple testing. *J R Stat Soc B Met* **57**, 289–300.
[27] Dennis Jr G, Sherman BT, Hosack DA, Yang J, Gao W, Lane HC, and Lempicki RA (2003). DAVID: database for annotation, visualization, and integrated discovery. *Genome Biol* **4**, P3.
[28] Szklarczyk D, Franceschini A, Wyder S, Forslund K, Heller D, Huerta-Cepas J, Simonovic M, Roth A, Santos A, and Tsafou KP, et al (2015). STRING v10: protein-protein interaction networks, integrated over the tree of life. *Nucleic Acids Res* **43**, D447–D452.
[29] Shannon P, Markiel A, Ozier O, Baliga NS, Wang JT, Ramage D, Amin N, Schwikowski B, and Ideker T (2003). Cytoscape: a software environment for integrated models of biomolecular interaction networks. *Genome Res* **13**, 2498–2504.
[30] Xiao F, Zuo Z, Cai G, Kang S, Gao X, and Li T (2009). miRecords: an integrated resource for microRNA-target interactions. *Nucleic Acids Res* **37**, D105–D110.
[31] Anaya J (2016). OncoLnc: linking TCGA survival data to mRNAs, miRNAs, and lncRNAs. *Peer J Comput Sci* **2**e67.
[32] Uhlen M, Zhang C, Lee S, Sjostedt E, Fagerberg L, Bidkhori G, Benfeitas R, Arif M, Liu Z, and Edfors F, et al (2017). A pathology atlas of the human cancer transcriptome. *Science* **357**.
[33] Malvezzi M, Carioli G, Bertuccio P, Boffetta P, Levi F, La Vecchia C, and Negri E (2017). European cancer mortality predictions for the year 2017, with focus on lung cancer. *Ann Oncol* **28**, 1117–1123.
[34] Larson A and Kwon RS (2017). Natural history of pancreatic cysts. *Dig Dis Sci* **62**, 1770–1777.
[35] Maisonneuve P, Amar S, and Lowenfels AB (2017). Periodontal disease, edentulism and pancreatic cancer: a meta analysis. *Ann Oncol* **28**, 985–995.
[36] Martinez-Useros J, Li W, Cabeza-Morales M, and Garcia-Foncillas J (2017). Oxidative stress: a new target for pancreatic cancer prognosis and treatment. *Nippon Rinsho*, 6.
[37] Boccardi M, Gallo V, Yasui Y, Vineis P, Padovani A, Mosimann U, Giannakopoulos P, Gold G, Dubois B, and Jack Jr CR, et al (2017). The biomarker-based diagnosis of Alzheimer's disease. 2-lessons from oncology. *Neurobiol Aging* **52**, 141–152.
[38] Kramer F, Sabbah HN, Januzzi JJ, Zannad F, Peter van Tintelen J, Schelbert EB, Kim RJ, Milting H, Vonk R, and Neudeck B, et al (2017). Redefining the role of biomarkers in heart failure trials: expert consensus document. *Heart Fail Rev* **22**, 263–277.
[39] Pilarsky C, Ammerpohl O, Sipos B, Dahl E, Hartmann A, Wellmann A, Braunschweig T, Lohr M, Jesenofsky R, and Friess H, et al (2008). Activation of Wnt signalling in stroma from pancreatic cancer identified by gene expression profiling. *J Cell Mol Med* **12**, 2823–2835.
[40] Winter C, Kristiansen G, Kersting S, Roy J, Aust D, Knosel T, Rummele P, Jahnke B, Hentrich V, and Ruckert F, et al (2012). Google goes cancer: improving outcome prediction for cancer patients by network-based ranking of marker genes. *PLoS Comput Biol* **8**e1002511.
[41] Jahny E, Yang H, Liu B, Jahnke B, Lademann F, Knosel T, Rummele P, Grutzmann R, Aust DE, and Pilarsky C, et al (2017). The G protein-coupled receptor RAI3 is an independent prognostic factor for pancreatic cancer survival and regulates proliferation via STAT3 phosphorylation. *PLoS One* **12**, e0170390.
[42] Collisson EA, Sadanandam A, Olson P, Gibb WJ, Truitt M, Gu S, Cooc J, Weinkle J, Kim GE, and Jakkula L, et al (2011). Subtypes of pancreatic ductal adenocarcinoma and their differing responses to therapy. *Nat Med* **17**, 500–503.
[43] Newhook TE, Blais EM, Lindberg JM, Adair SJ, Xin W, Lee JK, Papin JA, Parsons JT, and Bauer TW (2014). A thirteen-gene expression signature predicts survival of patients with pancreatic cancer and identifies new genes of interest. *PLoS One* **9**e105631.
[44] Pihlak R, Valle JW, and McNamara MG (2017). Germline mutations in pancreatic cancer and potential new therapeutic options. *Oncotarget* **8**, 73240–73257.
[45] Bailey P, Chang DK, Nones K, Johns AL, Patch AM, Gingras MC, Miller DK, Christ AN, Bruxner TJ, and Quinn MC, et al (2016). Genomic analyses identify molecular subtypes of pancreatic cancer. *Nature* **531**, 47–52.
[46] He D, Xiang J, Li B, and Liu H (2016). The dynamic behavior of Ect2 in response to DNA damage. *Sci Rep* **6**, 24504.
[47] Cook DR, Rossman KL, and Der CJ (2014). Rho guanine nucleotide exchange factors: regulators of Rho GTPase activity in development and disease. *Oncogene* **33**, 4021–4035.
[48] Mack NA and Georgiou M (2014). The interdependence of the Rho GTPases and apicobasal cell polarity. *Small GTPases* **5**, 10.
[49] Justilien V, Ali SA, Jamieson L, Yin N, Cox AD, Der CJ, Murray NR, and Fields AP (2017). Ect2-dependent rRNA synthesis is required for KRAS-TRP53-driven lung adenocarcinoma. *Cancer Cell* **31**, 256–269.
[50] Greer ER, Chao AT, and Bejsovec A (2013). Pebble/ECT2 RhoGEF negatively regulates the Wingless/Wnt signaling pathway. *Development* **140**, 4937–4946.
[51] Werner K, Lademann F, Thepkaysone ML, Jahnke B, Aust DE, Kahlert C, Weber G, Weitz J, Grutzmann R, and Pilarsky C (2016). Simultaneous gene silencing of KRAS and anti-apoptotic genes as a multitarget therapy. *Oncotarget* **7**, 3984–3992.

[52] Zhang ML, Lu S, Zhou L, and Zheng SS (2008). Correlation between ECT2 gene expression and methylation change of ECT2 promoter region in pancreatic cancer. *Hepatobiliary Pancreat Dis Int* **7**, 533–538.

[53] Dutta S, Roy S, Polavaram NS, Baretton GB, Muders MH, Batra S, and Datta K (2016). NRP2 transcriptionally regulates its downstream effector WDFY1. *Sci Rep* **6**, 23588.

[54] Fujii T, Shimada K, Asano A, Tatsumi Y, Yamaguchi N, Yamazaki M, and Konishi N (2016). MicroRNA-331-3p suppresses cervical cancer cell proliferation and E6/E7 expression by targeting NRP2. *Int J Mol Sci* **17**.

[55] Ng T, Hor CH, Chew B, Zhao J, Zhong Z, Ryu JR, and Goh EL (2016). Neuropilin 2 signaling is involved in cell positioning of adult-born neurons through glycogen synthase kinase-3beta (GSK3beta). *J Biol Chem* **291**, 25088–25095.

[56] Ou JJ, Wei X, Peng Y, Zha L, Zhou RB, Shi H, Zhou Q, and Liang HJ (2015). Neuropilin-2 mediates lymphangiogenesis of colorectal carcinoma via a VEGFC/VEGFR3 independent signaling. *Cancer Lett* **358**, 200–209.

[57] Domoto T, Pyko IV, Furuta T, Miyashita K, Uehara M, Shimasaki T, Nakada M, and Minamoto T (2016). Glycogen synthase kinase-3beta is a pivotal mediator of cancer invasion and resistance to therapy. *Cancer Sci* **107**, 1363–1372.

[58] Yasuoka H, Kodama R, Tsujimoto M, Yoshidome K, Akamatsu H, Nakahara M, Inagaki M, Sanke T, and Nakamura Y (2009). Neuropilin-2 expression in breast cancer: correlation with lymph node metastasis, poor prognosis, and regulation of CXCR4 expression. *BMC Cancer* **9**, 220.

[59] Uronis HE, Bendell JC, Altomare I, Blobe GC, Hsu SD, Morse MA, Pang H, Zafar SY, Conkling P, and Favaro J, et al (2013). A phase II study of capecitabine, oxaliplatin, and bevacizumab in the treatment of metastatic esophagogastric adenocarcinomas. *Oncologist* **18**, 271–272.

[60] Qiu WY, Zheng LB, Pan F, Wang BB, and Yao YF (2016). New histopathologic and ultrastructural findings in Reis-Bucklers corneal dystrophy caused by the Arg124Leu mutation of TGFBI gene. *BMC Ophthalmol* **16**, 158.

[61] Wang F, Hu W, Xian J, Ohnuma S, and Brenton JD (2013). The Xenopus Tgfbi is required for embryogenesis through regulation of canonical Wnt signalling. *Dev Biol* **379**, 16–27.